

# Modern Alchemical Free Energy Methods for Drug Discovery Explained

Darrin M. York\*

Cite This: *ACS Phys. Chem Au* 2023, 3, 478–491

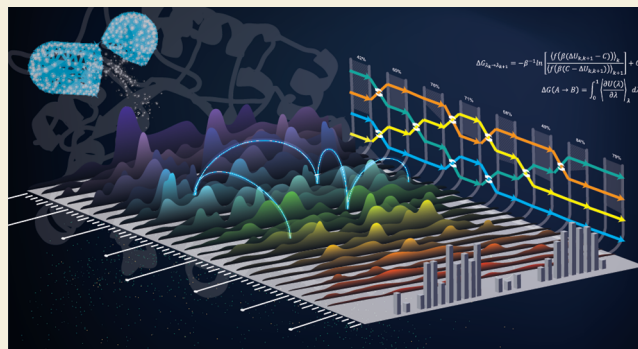
Read Online

ACCESS |

Metrics &amp; More

Article Recommendations

**ABSTRACT:** This Perspective provides a contextual explanation of the current state-of-the-art alchemical free energy methods and their role in drug discovery as well as highlights select emerging technologies. The narrative attempts to answer basic questions about what goes on “under the hood” in free energy simulations and provide general guidelines for how to run simulations and analyze the results. It is the hope that this work will provide a valuable introduction to students and scientists in the field.



**KEYWORDS:** drug design, lead optimization, binding free energy, molecular simulation, enhanced sampling

This Perspective is a treatise that brings together and describes the most critical components of alchemical free energy (AFE) methods and places them into the context of free energy simulations used in drug discovery. For broader discussion of methods in the field, the reader is referred to several excellent texts<sup>1,2</sup> and reviews.<sup>3–9</sup> This is an active field with a long history that can be difficult to navigate, especially for new students and practitioners.<sup>10</sup> This work endeavors to answer basic questions about what goes on “under the hood” in free energy simulations and is subjective in the sense that it draws from methods that have been developed in the author’s lab and implemented in the most recent AMBER suite of programs,<sup>11</sup> including emerging technologies available for testing as part of the AMBER Drug Discovery Boost package.<sup>12</sup>

## 1. WHAT IS AN ALCHEMICAL FREE ENERGY SIMULATION?

Molecular dynamics (MD) simulations<sup>13</sup> have been traditionally used to explore the equilibrium and dynamical properties of a *single state* of a system. Free energy simulations are a distinct class of simulations that explore a process whereby one state of the system changes into a different state.<sup>1</sup> In practice, this usually implies performing a series of simulations that sample both end states and usually the free energy surfaces and/or pathways connecting the states. There are two general categories of free energy simulations that have been subsequently described.

The first category is referred to as the “free energy surface” (FES) or “potential of mean force” (PMF) profile methods that explore a reduced-dimensional free energy profile along some

appropriate set of coordinates that describe the real chemical process being studied. Often a goal of these methods is to determine the minimum free energy pathways between states. The pathway establishes the mechanism for the chemical process and thus is of interest together with the free energy values along the path and the associated critical points (e.g., transition states and intermediates) from which kinetic parameters can be determined and predictions can be made. Example applications<sup>14</sup> include the study of catalytic mechanisms of enzymes,<sup>15,16</sup> transport of ions through membrane ion channels,<sup>17</sup> or folding of protein<sup>18</sup> or RNA<sup>19</sup> molecules. This method can also be used to study binding of small molecules in host–guest systems<sup>20</sup> or to biological targets<sup>21,22</sup> and has the advantage that it can provide estimates of on/off rates that may be correlated with drug potency.<sup>23</sup>

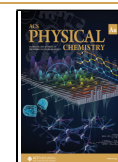
The second category is referred to as “alchemical free energy” methods<sup>24</sup> and is illustrated in Figure 1. Here the primary interest is in the overall free energy difference for the process and not the chemical mechanism itself. As the free energy is a state function, changes in free energy are independent of the path taken to effect the transition between states. AFE methods leverage artificial “alchemical” pathways that are more computa-

Received: July 17, 2023

Revised: September 12, 2023

Accepted: September 13, 2023

Published: October 4, 2023



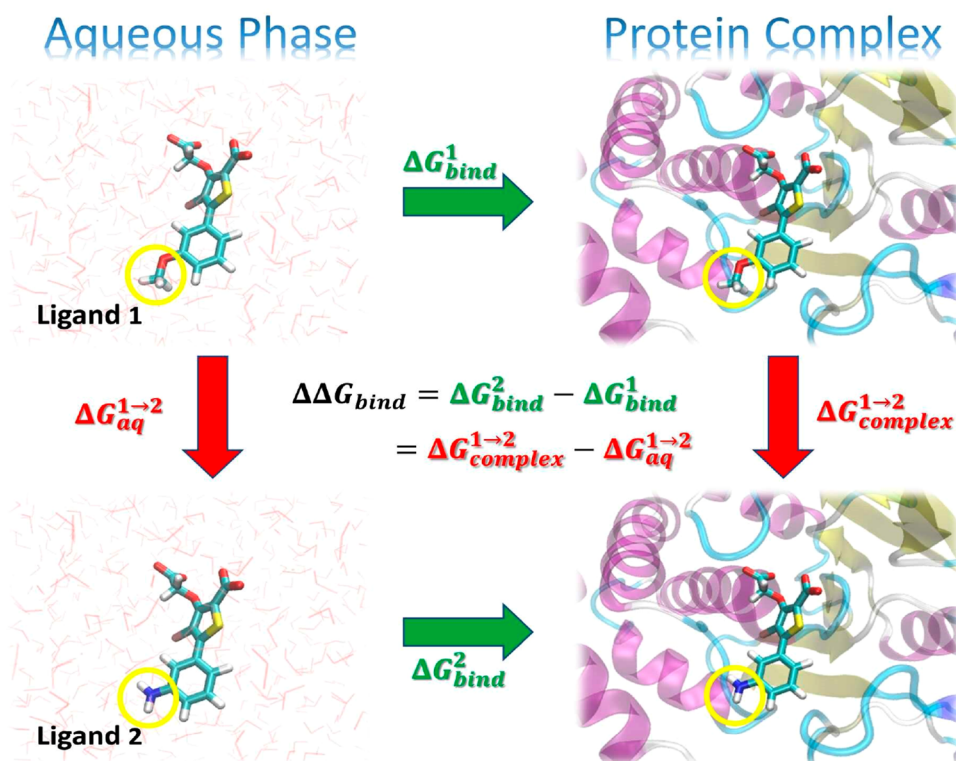


**Figure 1.** Illustration of a thermodynamic cycle for the relative binding free energy (RBEF,  $\Delta\Delta G_{\text{bind}}$ ) between two ligands (“Ligand 1” and “Ligand 2”). The green arrows represent the absolute binding free energy (ABFE,  $\Delta G_{\text{bind}}$ ) of each ligand (indicated by the superscript), which involves changing the environment from unbound in the aqueous phase to bound in a complex with the protein target. These quantities are experimentally measurable but are challenging to directly compute, as the change in the environment can be considerably complicated. The red arrows represent alchemical transformations where Ligand 1 is mutated into a similar Ligand 2 in the same environment. These transformations are frequently more amenable to practical computations. The yellow circles in the figures indicate the region of each ligand that undergoes the most significant changes in the alchemical transformation and would likely be modeled using a “softcore potential” during the alchemical transformation.

tionally efficient in determining the free energy differences between end states. In this way, one can gain efficiency and robustness in the computation of the free energy difference between states but at the cost of forfeiting information about the real chemical pathways connecting the states. Example applications include the transfer of a molecule from one environment to another (e.g., from the gas phase to aqueous solution), the change in protonation state of a titratable residue in a protein or nucleic acid, or the binding of a drug-like molecule (ligand) to a protein target<sup>4</sup> (as is the focus of this Perspective).

Formally, these two categories of methods share common theoretical foundations in statistical mechanics and methods for their solution when one recognizes that the main difference is in the choice of real (chemical) or artificial (alchemical) pathways used to connect states. In this way, many of the exact same underlying techniques can be used for either the FES or AFE simulations. For example, for either category one can perform simulations at a set of fixed (constrained) values along the pathway<sup>25</sup> such that the mean values of the derivatives (forces) at each point along the path can be numerically integrated to obtain the change in free energy as the reversible work. In the FES category, this is referred to as a PMF calculation,<sup>26</sup> whereas in the AFE category this is referred to as a thermodynamic integration (TI) calculation.<sup>27,28</sup> Alternatively, one can monitor fluctuations of the pathway coordinates use biasing potentials (e.g., in a set of “umbrella sampling” simulations<sup>29</sup>) and reassemble the free energy profile from these multiple distributions using variational approaches such as the unbinned

weighted histogram analysis method<sup>30</sup> (UWHAM), Bennett’s acceptance ratio (BAR)<sup>31</sup> or its multistate generalization (MBAR)<sup>32,33</sup> or network-wide extensions with cycle closure,<sup>34</sup> and variational free energy profile<sup>35–37</sup> (vFEP) methods. In the first category, these are known as biased sampling/free energy profile methods<sup>26,37,38</sup> (e.g., “umbrella sampling” and metadynamics<sup>39,40</sup>), whereas in the second category, this approach is encompassed in so-called  $\lambda$ -dynamics.<sup>41,42</sup> The take-home message here is that FES and AFE methods have the same foundational underpinnings, and most methods developed for one category can be transferred in some way to the other.

## 2. HOW ARE AFE SIMULATIONS USED IN DRUG DISCOVERY?

Computational predictions are a vital part of drug discovery, and with increasing access to high-performance computing, together with advances in machine learning technology, the role of these predictions in computer-aided drug design is increasing at a rapid pace. Arguably, the most rigorous and, in principle, most accurate of these methods are AFE simulations for prediction of the binding affinity of ligands (e.g., small drug-like molecules) to their macromolecular (e.g., protein or RNA) targets. Drug discovery companies use AFE simulations in the lead optimization phase to predict the RBEFs of proposed ligands and design selectivity to circumvent off-target effects.<sup>9</sup> Predictions are used to prioritize compounds for the next stage of development:<sup>3</sup> costly synthesis and testing in the lead optimization cycle, followed by preclinical drug development

and, if successful, advancement to clinical trials. As only a small fraction of trial compounds make it to approved drugs (with an average cost of getting a new drug to market of over \$1 billion),<sup>43</sup> even small increases in the accuracy of design predictions will have great impact on the cost and efficiency of drug development.<sup>44,45</sup>

### 3. WHAT ARE THE DIFFERENT WAYS WE CAN COMPUTE ALCHEMICAL FREE ENERGIES?

The change in free energy between two thermodynamic states can be rigorously computed using a free energy perturbation<sup>46</sup> (FEP) or TI<sup>27,28</sup> formulation or through nonequilibrium work (NEW) simulations using the Jarzynski equality<sup>47</sup> and its equation variations.<sup>48–54</sup> Both the TI and NEW approaches require the formulation of a transformation pathway between states in order to connect them. Only the FEP approach formally requires performing simulations only of one or both of the thermodynamic end states in order to obtain the free energy differences between the states. However, the “end-state-only” FEP approach is only reliable in practice if the two end states have large phase space overlap<sup>55–58</sup> (e.g., as in so-called indirect reference potential “book-ending” approaches;<sup>58</sup> see below). For ligand–protein binding, the FEP approach requires breaking down the pathway into smaller  $\lambda$  intervals, similar to the TI method. It should be noted that there exist other *approximate* (nonrigorous) “end-state-only” methods that require sampling only at the two thermodynamic end points, such as the MM-GB/SA, MM-PB/SA,<sup>59</sup> and LIE<sup>60</sup> methods, which are not discussed in this Perspective.

Hence, for drug discovery applications, the TI, FEP, and NEW methods all require a parametric pathway to be introduced to connect thermodynamic states. Often the parameter in this path is designated by the variable  $\lambda$  and varies between 0 and 1. As the end states are generally chemically distinct molecules with different compositions, the pathway is nonphysical and hence referred to as an “alchemical” transformation. This is achieved by defining a  $\lambda$ -dependent potential energy function  $U(\mathbf{r}^N; \lambda)$ , where  $U(\mathbf{r}^N; 0) = U_0(\mathbf{r}^N)$  and  $U(\mathbf{r}^N; 1) = U_1(\mathbf{r}^N)$  are the end-state potential energy functions (e.g., think of them as representing the “Ligand 1” and “Ligand 2” states in Figure 1), and the parameter  $\lambda$  transforms state 0 into state 1 in such a way as to be continuously differentiable in the interval  $[0, 1]$  (e.g., as depicted by the vertical red arrows in Figure 1). Here the coordinate  $\mathbf{r}^N$  represents the  $N$  Cartesian coordinates for each particle as well as any lattice vector information that defines the periodic boundary conditions for the system. While the free energy is a state function and formally is invariant to the pathway connecting states, in practice the TI, FEP, and NEW methods are all extremely sensitive to the pathway and the phase space overlap<sup>55–58</sup> of states along the pathway.

#### Thermodynamic Integration

In the TI method, the free energy change,  $\Delta A_{0 \rightarrow 1}$ , between states “0” and “1” can be achieved through integration of the thermodynamic derivative as

$$\begin{aligned} \Delta A_{0 \rightarrow 1} &= \int_0^1 d\lambda \left( \frac{dA}{d\lambda} \right) = \int_0^1 d\lambda \left\langle \frac{\partial U(\mathbf{r}^N; \lambda)}{\partial \lambda} \right\rangle_{\lambda} \\ &\approx \sum_{k=1}^M w_k \left\langle \frac{\partial U(\mathbf{r}^N; \lambda)}{\partial \lambda} \right\rangle_{\lambda_k} \end{aligned} \quad (1)$$

where the second integral involves the derivative of the potential energy  $U$  with respect to the parameter that smoothly connects the end states  $\lambda = 0$  and 1 and the averaging brackets indicate equilibrium sampling of the state characterized by subscript  $\lambda$ . For each  $\lambda$ -window “ $\lambda_k$ ”, mean values of  $\left\langle \frac{\partial U}{\partial \lambda} \right\rangle_{\lambda_k}$  are collected,

and the sum in eq 1 indicates numerical integration over  $M$  quadrature points  $\lambda_k$  ( $k = 1, \dots, M$ ) with associated weights  $w_k$ . The weights can be chosen in accord with a particular quadrature, such as the trapezoidal rule, Simpson’s rule, or various Gaussian quadrature rules.<sup>61</sup> Alternatively, spline functions<sup>61</sup> (e.g., cubic splines) or polynomials<sup>62</sup> can be fitted to the  $\left\langle \frac{\partial U}{\partial \lambda} \right\rangle$  profiles and integrated analytically.

#### Free Energy Perturbation

In the FEP method, the free energy change can be computed as

$$\Delta A_{0 \rightarrow 1} = \sum_{k=1}^{M-1} \Delta A_{\lambda_k \rightarrow \lambda_{k+1}} \quad (2)$$

where  $\lambda_k < \lambda_{k+1}$ ,  $\lambda_1 = 0$ , and  $\lambda_M = 1$ . The interval free energy change  $\Delta A_{\lambda_k \rightarrow \lambda_{k+1}}$  can be computed from one of several FEP equation variations given by

$$\Delta A_{\lambda_k \rightarrow \lambda_{k+1}} = -\beta^{-1} \ln \langle e^{-\beta \Delta U_{k,k+1}} \rangle_{\lambda_k} \quad (3)$$

designated “forward” exponential averaging,

$$\Delta A_{\lambda_k \rightarrow \lambda_{k+1}} = \beta^{-1} \ln \langle e^{\beta \Delta U_{k,k+1}} \rangle_{\lambda_{k+1}} \quad (4)$$

designated “reverse” exponential averaging, or

$$\Delta A_{\lambda_k \rightarrow \lambda_{k+1}} = -\beta^{-1} \ln \left[ \frac{\langle f(\beta(\Delta U_{k,k+1} - C)) \rangle_k}{\langle f(\beta(C - \Delta U_{k,k+1})) \rangle_{k+1}} \right] + C \quad (5)$$

designated as the “BAR” method, where  $\Delta U_{k,k+1} = U(\mathbf{r}^N; \lambda_{k+1}) - U(\mathbf{r}^N; \lambda_k)$ ,  $\beta = (k_B T)^{-1}$  is the inverse temperature (where  $k_B$  is the Boltzmann constant and  $T$  the absolute Kelvin temperature),  $f(x) = 1/(1 + e^x)$  is a Fermi function, and  $C$  is an arbitrary constant. Formally these expressions are equivalent in the limit of infinite sampling. The first and second expressions require conformation sampling (simulation) from one of the two end states of the interval  $[\lambda_k, \lambda_{k+1}]$  (as indicated by the subscript on the averaging bracket) and are sometimes referred to as the Zwanzig equation<sup>46</sup> or “exponential averaging”. The third expression is the BAR equation<sup>31</sup> and requires sampling from both end states and solving for  $C$  such that the first term vanishes (by equating the numerator and denominator) in order that  $C$  becomes the statistical best (minimal variance) estimate of the free energy  $\Delta A_{\lambda_k \rightarrow \lambda_{k+1}}$  for the interval. For MBAR<sup>32,33</sup> analysis, FEP data consist of an  $M \times M$  matrix of  $\Delta U_{k,k'}$  values ( $k, k' = 1, \dots, M$ ) for each sampling time point (noting that the diagonal values of this matrix are zero).

In principle, the FEP formula (eq 2) can be applied without taking recourse into intermediate  $\lambda$  states; i.e., in the limit that  $M = 2$ , only the end states  $\lambda = 0$  and/or 1 need to be sampled (no intermediate  $\lambda$ -window simulations are required). However, in practice, this “end-state-only” approach is only feasible if there is a very high degree of phase space overlap<sup>55–58</sup> between the  $\lambda = 0$  and 1 states (which is not the case for AFE simulations in drug discovery). Nonetheless, this can be an attractive approach when one wishes to correct a free energy obtained from simulations performed by using a “low-level” (computationally efficient)

Hamiltonian to a “high-level” (computationally intensive) Hamiltonian while avoiding the need to perform an expensive simulation at the high level. These end-state-model Hamiltonian corrections are sometimes referred to as “book-ending” corrections<sup>58</sup> (as part of an “indirect” AFE approach<sup>49,53,63–65</sup>) and typically have only modest sampling requirements because the chemical identity of the species does not change, just the potential energy model. Even so, often an intermediate low-level “reference potential” is still needed in order to achieve sufficient phase space overlap for the calculations to be reliable by considering only the end states,<sup>58</sup> or alternatively, non-equilibrium methods have been shown to be promising<sup>49,53,63–65</sup> (see below). The take-home message here is that for AFE calculations typically encountered in drug discovery (not “book-ending” corrections), the FEP approach requires simulations of intermediate  $\lambda$  states ( $\lambda$ -windows) with essentially the same requirements as for the TI method.

### Nonequilibrium Work

In the NEW methods, the free energy change is computed from a series of nonequilibrium simulations where the work is calculated for transforming  $\lambda$  from 0 to 1 over a time interval  $\tau$ . Here, by “nonequilibrium” simulations it is recognized that the time interval is not sufficiently long that it can be assumed that the system has reached equilibrium at every sampled  $\lambda$  value in the interval  $0 \leq \lambda \leq 1$ . Let us define the work of such a transformation that departs from starting coordinates  $\mathbf{r}^N(0) = \mathbf{r}_0^N$  at  $t = 0$  and takes place over the time interval  $[0, \tau]$  as

$$\mathcal{W}(\mathbf{r}_0^N; \tau) = \int_0^\tau \frac{\partial U(\mathbf{r}^N; \lambda)}{\partial \lambda} \cdot \frac{d\lambda(t)}{dt} dt \quad (6)$$

where in the integral both the coordinates  $\mathbf{r}^N$  and  $\lambda$  are functions of time and it is implicit that  $\lambda$  will vary from 0 to 1 over the time interval. If one sets the  $d\lambda/dt$  rate to be constant over the interval (i.e.,  $d\lambda/dt = 1/\tau$ ), then the above equation simplifies to

$$\begin{aligned} \mathcal{W}(\mathbf{r}_0^N; \tau) &= \frac{1}{\tau} \int_0^\tau \frac{\partial U(\mathbf{r}^N; \lambda)}{\partial \lambda} dt \\ &= \left\langle \frac{\partial U(\mathbf{r}^N; \lambda)}{\partial \lambda} \right\rangle_{\{\mathbf{r}_0^N, \tau\}} \end{aligned} \quad (7)$$

Here the subscripts  $\{\mathbf{r}_0^N, \tau\}$  on the averaging brackets emphasize that the average is taken from a nonequilibrium simulation of duration  $\tau$  departing from initial coordinates  $\mathbf{r}_0^N$ . In order to calculate the free energy  $\Delta A_{0 \rightarrow 1}$ , one performs a series of short nonequilibrium work simulations by sampling the initial conditions  $\{\mathbf{r}_0^N\}$  from the *equilibrium end-state distribution(s)*, and computes the free energy change analogously to eqs 3–5:

$$\Delta A_{0 \rightarrow 1} = -\beta^{-1} \ln \langle e^{-\beta \mathcal{W}(\mathbf{r}_0^N; \tau)} \rangle_0 \quad (8)$$

$$\Delta A_{0 \rightarrow 1} = \beta^{-1} \ln \langle e^{\beta \mathcal{W}(\mathbf{r}_0^N; \tau)} \rangle_1 \quad (9)$$

$$\Delta A_{0 \rightarrow 1} = -\beta^{-1} \ln \left[ \frac{\langle f(\beta(\mathcal{W}(\mathbf{r}_0^N; \tau) - C)) \rangle_0}{\langle f(\beta(C - \mathcal{W}(\mathbf{r}_0^N; \tau))) \rangle_1} \right] + C \quad (10)$$

where the subscripts in the averaging brackets indicate the equilibrium end state distribution from which the initial conditions are sampled for the nonequilibrium simulations. Equation 8 was the original equality proven by Jarzynski,<sup>47</sup> from which much work has followed, including the formula developed by Crooks<sup>48</sup> (eq 10).

The nonequilibrium work free energy formulation forms an elegant connection between the thermodynamic integration and free energy perturbation formulas. In the limit that the nonequilibrium work simulation is performed over an infinite amount of time, such that the equilibrium work is actually measured (and the results become independent of initial conditions and do not require averaging), the above formulas become identical to the thermodynamic integration formula of eq 1:

$$\lim_{\tau \rightarrow \infty} \mathcal{W}(\mathbf{r}_0^N; \tau) = \int_0^1 d\lambda \left\langle \frac{\partial U(\mathbf{r}^N; \lambda)}{\partial \lambda} \right\rangle_\lambda = \Delta A_{0 \rightarrow 1} \quad (11)$$

Alternatively, in the limit that the nonequilibrium work is performed over a vanishingly short amount of time, such that the coordinates  $\mathbf{r}^N$  remain fixed, the above formula becomes identical to the change in potential energy:

$$\lim_{\tau \rightarrow 0} \mathcal{W}(\mathbf{r}^N; \tau) = \Delta U_{0,1}(\mathbf{r}^N) \quad (12)$$

where  $\Delta U_{0,1}(\mathbf{r}^N) = U(\mathbf{r}^N; 1) - U(\mathbf{r}^N; 0)$ . In this limit, substitution of eq 12 into the nonequilibrium work free energy equations (eqs 8–10) recovers the free energy perturbation equations (eqs 3–5).

## 4. WHAT IS THE BEST METHOD TO USE: FEP (BAR/MBAR), TI, OR NEW?

The conservative, and perhaps less satisfactory answer to this question is almost universally “it is case-dependent”, as each method has advantages and disadvantages. The more aggressive answer is “use more than one method at the same time and perform consistency checks”. What follows is a short discussion of various pros and cons of the different methods as well as general recommendations for establishing robust best practices.

### TI versus FEP (BAR/MBAR)

The FEP and TI methods are closely related and have similar computational requirements, and for most codes the overhead for calculating TI, BAR, and MBAR free energy estimates at the same time is negligible. MBAR statistics for a particular  $\lambda$ -window  $k$  requires evaluation of  $\Delta U_{k,k'}$  at other  $\lambda$ -windows  $k' \neq k$ . Not all pairs of state distributions (i.e., not all possible  $k' \neq k$ ) need to be considered in the MBAR analysis (e.g., one could consider only  $|k' - k| \leq n$  in the analysis, where  $n$  is an integer representing the number of nearest-neighbor  $\lambda$ -windows). In the BAR method, only intervals between nearest-neighbor  $\lambda$ -windows are considered. The traditional TI method, on the other hand, requires  $\partial U/\partial \lambda$  statistics only for the  $\lambda$ -window being sampled (although methods have been proposed that enable additional statistics to be collected at neighboring  $\lambda$ -windows as well<sup>66</sup>). For well-behaved calculations, MBAR is often the most rapidly convergent of the methods; however, for edge cases, BAR may be more robust. In other cases, the exponential term in the integrand of the FEP (BAR/MBAR) methods can become unstable and more difficult to average due to large fluctuations in the  $\Delta U_{k,k'}$  values, whereas the  $\partial U/\partial \lambda$  integrand in the TI method may be less sensitive and yield more stable averages. In any case, the statistical quantities required for the BAR, MBAR, and TI methods are not prohibitive to compute at the same time (as they typically only have to be collected every 1000 time steps or so). It is thus recommended that free energies be calculated from all three analysis methods and used as a consistency check that can help to flag potential

problematic edge cases. If, for example, the differences between TI, BAR, and MBAR free energy values are larger than their corresponding statistical error estimates, then likely there is a problem in the calculation that needs to be addressed (see below).

### TI/FEP versus NEW

As mentioned previously, the NEW methods form a conceptual connection between the TI and FEP methods, but aspects of their practical application can be different. NEW methods have been successfully applied to a number of problems, most notably single-molecule force microscopy<sup>67</sup> and related physical and chemical processes and MM  $\rightarrow$  QM transformations in “book-ending” corrections.<sup>49,53,63–65</sup> Only fairly recently have NEW methods seen application in direct AFE simulations for drug discovery,<sup>68</sup> and hence, they are currently less mature than TI and FEP methods and have less well-demonstrated behavior. NEW calculations critically depend on the ability to first sufficiently sample the equilibrium end state distributions that are then used to launch short nonequilibrium switching simulations. The switching time, together with the number of switches (i.e., the number of initial conditions sampled from the equilibrium end state distribution), determines the reliability of the resulting free energy estimate. In practice, the switching time depends on how quickly the environment is able to relax and accommodate the  $\lambda$  perturbation and how much this relaxation affects the free energy estimate. These properties can vary widely between aqueous and protein environments and even more so between relative and absolute binding free energy calculations, often in ways that are not easily predictable. These issues notwithstanding, a computational advantage of the NEW methods is that the ensemble of switching simulations are all independent of one another and can be performed in parallel. As the switching simulations are themselves short with respect to those needed by TI and FEP methods, this can translate into potentially very short wall-clock turnaround for users that have substantial on-demand parallel resources such as are available on the cloud (albeit for a high price tag). However, a significant advantage of current TI and FEP methods over the NEW methods is that the former are easily integrated with modern enhanced equilibrium sampling methods such as the ACES<sup>69</sup> approach discussed below. It is likely that as NEW approaches for AFE calculations continue to evolve they will become an increasingly important tool. As the field is still in the early stages in this regard, the remainder of this Perspective will focus on practical aspects of the more established equilibrium TI and FEP approaches used for drug discovery applications.

## 5. WHAT ARE THE CONSIDERATIONS THAT GO INTO PERFORMING A SET OF AFE SIMULATIONS?

There are many steps that go into a setting up AFE simulations in a drug discovery workflow,<sup>4</sup> ranging from developing structural models for the protein target (if full experimental structures have not been determined at sufficiently high resolution) and ranking docking poses for proposed ligands at the start to making predictions about off-target binding in order to engineer selectivity. In this Perspective, discussion is focused on AFE simulations (RBFE or ABFE) for a set of ligands binding to a single protein target, where the presumed starting point is that reliable starting structures have been prepared for each ligand–protein complex and relaxed and equilibrated in a realistic solvated environment under relevant conditions of temperature, pressure, pH, and ionic strength. The same starting

point must also exist for the unbound ligands in aqueous solution as part of the thermodynamic cycle (Figure 1) and, in the case of ABFE calculations, also the unbound (apo) state of the target. To arrive at such a starting point requires practical considerations that have been discussed in detail elsewhere<sup>4,70,71</sup> and are now only briefly mentioned.

First, one should endeavor to depart from a high-fidelity structure of the protein (or other biological target molecule) obtained from experiment (e.g., X-ray crystallography, NMR, or cryo-EM), preferably in ligand-bound form so as to provide information about the ligand binding mode and any target rearrangement that might be induced upon binding. If such structures are not available, then recourse can be taken into homology or integrative structural modeling<sup>72–74</sup> or computational predictions (e.g., Rosetta<sup>75</sup> or AlphaFold2<sup>76,77</sup>). In real-world drug discovery applications, it is unlikely that structures exist for the ligand–protein complexes for which binding affinities are to be predicted, and initial structures typically come from docking and scoring procedures<sup>77–81</sup> or alignment of ligands of a congeneric series with the known structure of the most chemically similar cocrystallized ligand based on shape similarity, followed by energy refinement.<sup>71</sup> The next goal is to generate a reliable model of the conformational ensemble in a realistic environment under relevant temperature, pressure, pH, and ionic strength conditions. Here it is important to ensure that all residues and functional groups of both ligands and target are in their most probable tautomeric form/protonation state<sup>82</sup> (which may differ in different environments). Further, it is important to include placement of key water molecules and ions, e.g., solvent components observed crystallographically or predicted by computational methods.<sup>83–86</sup> One common mistake made in calculations is to neutralize a charged protein or nucleic acid with only minimal counterions, as opposed to additionally adding a background of (counterion/co-ion) salt at relevant concentration (e.g., 0.14 M). Not only is this unrealistic, it is also more difficult to sample.<sup>87,88</sup> Once the solvation environment has been established, carefully controlled molecular dynamics procedures using appropriate force fields for the target, ligands, and solvation environment are typically used to allow relaxation of the solvent and ultimately the ligand/target structures (e.g., from their experimental crystal environments) to aqueous solution under constant temperature and pressure conditions. As more than half of drug targets are membrane proteins, additional considerations are needed for AFE simulations in these more complex heterogeneous environments.<sup>89–91</sup>

Once the individual ligand–protein complexes have been prepared and equilibrated in a realistic environment under relevant conditions, AFE simulations can be performed to obtain the relative or absolute binding free energy. This is the main focus of the current Perspective. The following are decisions the practitioner needs to make prior to setting out to run a set of AFE calculations:

- How to construct the thermodynamic graph network.
- How to define the alchemical transformation pathways.
- How to optimize alchemical enhanced sampling.

Each of these is considered in more detail below. It should be emphasized that for each of these topics, there are different strategies that can be taken and different methods that can be brought to bear to solve the problem. In the present discussion, emphasis is placed on those methods for which the author has had first-hand experience in developing and/or applying.

Nonetheless, there are alternative methods and approaches that are likely equally effective but that are not reviewed here.

### 5.1. How to Construct the Thermodynamic Graph Network

The construction of thermodynamic graph networks is a topic for which there are many different strategies.<sup>92</sup> Early strategies built upon the idea that networks of ligands would be connected using a minimal spanning tree (smallest number of edges) to reduce computational cost, and the edges would be chosen to avoid large perturbations (i.e., connect/transform the most structurally similar ligands). In such transformations, a maximum common substructure<sup>93</sup> between two ligands was often identified to define the atom mapping procedure, i.e., the mapping of each atom in one ligand to a structurally similar atom in the second ligand (the equivalent mapped atoms would usually share the same coordinates during the transformation). By maximizing the common substructure, the number of remaining atoms would be minimized. These atoms would have to be either created or annihilated in the transformation and often required the use of specialized “softcore” potentials and treatment with separable coordinates during the transformation.

With the concurrent advancement of new AFE methods, high-performance computing hardware, and efficient software implementations, this once established paradigm is now being revisited to some degree. As will be discussed in more detail below, the construction of more “dense” thermodynamic graph networks<sup>94</sup> enables analysis of cycle closure conditions as well as integration of experimental free energy constraints for known ligands. Network AFE simulations can be performed adaptively with resources allocated dynamically in order to improve precision of the free energy predictions.<sup>95,96</sup> Further, the choice of atoms treated by softcore potentials and using a dual topology are leveraged in alchemical enhanced sampling methods such as ACES.<sup>69</sup> Hence, while large perturbations should still be avoided if possible, it is sometimes advantageous to choose a smaller “common substructure” or “common core” region (and hence a larger region treated with softcore potentials and separate coordinates within the dual topology) in order that flexible substituents (such as functional groups or rings attached to the common core by single bonds) can be selected for enhanced sampling. These will be discussed in more detail below.

**RBFE or ABFE?** When constructing a thermodynamic graph network, one consideration is whether to use relative or absolute binding free energy calculations or a combination of the two. In the case of ABFE calculations, the entire ligand is in some way “annihilated”, or more precisely, it is transformed into a noninteracting “dummy atom” state,<sup>97–99</sup> which creates a void space that the environment must then strive to fill during the transformation. Further, specialized restraints need to be imposed in the dummy state such that the noninteracting ligand remains bound in the pocket so that it will retain better phase space overlap with the neighboring  $\lambda$  states.<sup>100,101</sup> One might naively argue that ABFE calculations are more preferable as they are not subject to “cycle closure conditions”, as are RBFE calculations in thermodynamic graph networks that contain redundancies in path connections. However, the reality is that ABFE simulations are much more computationally intensive, as the nature of the transformations is much larger, and the fact that the consistency of results cannot be checked with cycle closure conditions is a significant concern rather than an advantage of the method.

RBFE calculations, on the other hand, enable dense thermodynamic graphs to be constructed and cycle closure conditions to be leveraged to increase overall calculation precision and potentially accuracy as well in the case of inclusion of experimental free energy constraints for known ligands.<sup>34,94</sup> When RBFE calculations are being performed optimally, there is only modest rearrangement of the environment along the alchemical transformation pathway and minimal generation of void space that needs to be occupied by the environment. Moreover, RBFE simulations do not have the same issues as ABFE simulations of maintaining position in the binding pocket when the ligand is in the pure dummy atom state, as such a state does not exist for the RBFE case where there is a shared “common core” of atoms.<sup>102</sup> Alternatively stated, as the two ligand real-state end points are stably bound in an RBFE simulation, the corresponding partial dummy state ligand also will remain bound, as it shares a common core of atoms with the bound ligand that prevents it from diffusing away.

In some cases, RBFE calculations can be performed even when the ligands do not share a “common core” (where atoms in one ligand cannot be directly mapped into those of the other) but are nonetheless similar in overall shape and binding mode (i.e., there is substantial overlap of the ligand shapes and excluded volumes). In this situation, one can perform RBFE simulations as counterpoised ABFE simulations,<sup>103</sup> i.e., two ABFE transformations performed in opposite directions along the  $\lambda$  dimension within the same simulation. This method will retain the advantage that there is minimal relaxation of the environment and need to occupy void space that is created during the transformation; however, as the ligands no longer share a common core of atoms, Boresch-type restraints<sup>100,101</sup> must be imposed to prevent the dummy atom states<sup>99</sup> from drifting out of the binding pocket. This form of RBFE calculation between ligands that do not share a common core will be referred to as “core-hopping RBFE”.

Hence, the following is a hierarchy of complexity of AFE calculations of ligands and recommendations of what type of calculation (RBFE, core-hopping RBFE, or ABFE) to perform:

- RBFE: For transformations between ligands that share a common core of atoms (molecular scaffold), such as a congeneric series, and have similar binding modes, i.e., the ligands have strongly overlapping shapes and excluded volumes when bound.
- Core-hopping RBFE: For transformations between ligands that do not share a common core of atoms (molecular scaffold) but have similar shapes and binding modes, i.e., the ligands have strongly overlapping excluded volumes when bound but lack a straightforward atom mapping to a common core.
- ABFE: For transformations of a single ligand for which no other ligand has a similar shape and binding mode, i.e., no other ligand has a strongly overlapping excluded volume when bound.
- ABFE: For transformations of a single representative ligand within a subnetwork of RBFE calculations such that the relative binding free energy values can be connected to those of other ligand subnetworks for which RBFE calculations between subnetworks are not practical (e.g., that have different/nonoverlapping binding modes).

It should be mentioned that there are emerging methods that may further modify the above paradigm. One such promising method is the alchemical transfer method (ATM),<sup>104</sup> a novel

approach based on a coordinate transformation that swaps the positions of two ligands. The method has been tested successfully on ligands with diverse scaffolds and offers the advantage of being applicable with any potential energy function.<sup>105,106</sup>

## 5.2. How to Define the Alchemical Transformation Pathways

There are many strategies for performing free energy simulations<sup>4,8,107</sup> and in turn for choosing appropriate alchemical transformation pathways. Here the focus is on “concerted” alchemical transformations (sometimes referred to as “one-step” or “unified” procedures) where all nonbonded terms (e.g., electrostatic and Lennard-Jones) occur synchronously. This differs from “stepwise” transformations (sometimes referred to as “multistep” or “split” procedures), where transformation of electrostatic and Lennard-Jones terms occur asynchronously, for example, in a three-step “discharge/LJ/recharge” transformation. Concerted transformations are particularly useful in RBEF calculations, as they avoid weakly bound states that may require additional restraints and are easily integrated with enhanced sampling tools such as replica exchange and ACES. Formally, the lines that separate concerted and stepwise transformations are somewhat arbitrary and can be tuned by so-called “ $\lambda$ -scheduling”, where different energy terms can be turned off/on independently over different subintervals of the global  $[0, 1]$   $\lambda$  interval.<sup>12,102</sup>

Alchemical free energy simulations typically require at least some atoms to be effectively created or annihilated during the transformation process. This is achieved by transforming atoms into so-called “dummy atoms”<sup>97–99</sup> that do not interact with the real atoms of the physical system except through select bonded interactions such that they do not introduce a net potential of mean force on any of the real atoms. Transformations of real atoms into dummy atoms can be especially challenging if there is poor phase space overlap of neighboring states along the transformation coordinate,<sup>56,58,99,108,109</sup> giving rise to chronic problems such as end-point catastrophes, particle collapses, and large gradient jumps.<sup>102</sup> This issue can also occur in transformations between two real atoms that have significantly different force field parameters.

A number of strategies have been explored to develop stable transformation pathways in alchemical free energy simulations, including the use of so-called “softcore potentials” with separation-shifted scaling,<sup>110–112</sup> parameter interpolation,<sup>113</sup> short-range switching,<sup>114</sup> or capping the short-range interactions<sup>115,116</sup> and nonlinear mixing of the end-point potentials.<sup>117–121</sup> Recent studies have shown that adverse effects of these problematic transitions can lead to large variance and in some cases order/disorder transitions along the alchemical path that can hinder sampling and convergence of free energy estimates.<sup>116</sup> Very recently, a  $\lambda$ -enveloping distribution sampling method,<sup>107,122,123</sup> which is related to approaches to optimize minimum-variance pathways in alchemical transformations,<sup>124–126</sup> has been explored as an alternative coupling scheme to more conventional  $\lambda$ -intermediate states.

Recently, we developed a new framework<sup>12</sup> for the design of optimized alchemical transformation pathways.<sup>127</sup> The methods extended and improved the use of so-called “smoothstep” softcore potentials<sup>128</sup> to address chronic problems of particle collapse and large gradient jumps.<sup>127</sup> Important improvements include (1) consistent power scaling of Coulomb (Coul) and Lennard-Jones (LJ) interactions with unitless control param-

eters to maintain balance of electrostatic attractions and exchange repulsions, (2) introduction of a pairwise form based on the LJ contact radius for the effective interaction distance with separation-shifted scaling, and (3) rigorous smoothing of the softcore potential at the nonbonded cutoff boundary. The new softcore potentials and optimized alchemical transformation pathways<sup>127</sup> improve phase space overlap between neighboring states and have been leveraged in the development of the new alchemical enhanced sampling (ACES) method<sup>69</sup> for accelerated convergence of conformational ensembles and free energy estimates.

## 5.3. How to Optimize Alchemical Enhanced Sampling

The term “enhanced sampling” has been used in many contexts.<sup>129–137</sup> As the dynamic degrees of freedom in a molecular simulation are usually the atomic positions, sampling is intimately connected to different conformations of the system. It is important to distinguish “conformational sampling” of a target distribution from “conformational searching” for a structural ensemble or pathway that optimally satisfies some property of interest that is part of the search criteria (e.g., a stable docking pose, metal ion binding site, or protein/nucleic acid conformational state). In the context of free energy simulations, enhanced sampling implies sampling in regions that contribute substantially to the free energy change of interest but that are only seldom visited by Boltzmann sampling (e.g., by conventional molecular dynamics) of any one state along the transformation pathway. This subclass of methods is referred to as “importance sampling” methods. As an example, if a ligand can adopt multiple orientations in the binding pocket of a protein, then a method able to sample each with the correct occupation is important to obtain an accurate estimate of the binding free energy. On the other hand, an enhanced sampling method used to study protein folding pathways that explore conformations of folded and unfolded states likely would be counterproductive to the sampling needed to converge the free energy estimate for ligand–protein binding where only the folded state significantly contributes. In this sense, importance sampling must focus on the degrees of freedom responsible for converging the free energy change of interest while avoiding unnecessary “enhanced sampling” of other degrees of freedom.<sup>1,138</sup>

There is a vast array of enhanced sampling methods for AFE simulations,<sup>129–132,132–136,139,140</sup> including replica exchange (RE)<sup>141–143</sup> and multiple-replica strategies that use adaptive biasing forces,<sup>144</sup> umbrella sampling (US),<sup>29,145</sup> parallel or simulated tempering,<sup>141,142,146,147</sup> metadynamics,<sup>148</sup> self-guided molecular dynamics,<sup>149</sup> replica exchange with solute tempering (REST<sup>150</sup> or REST2<sup>151</sup>), multicanonical algorithm (MUCA),<sup>152–154</sup> orthogonal space random walk (OSRW),<sup>155</sup>  $\lambda$ -enveloping distribution sampling (EDS/ $\lambda$ -EDS),<sup>122,123,156</sup> thermodynamic integration with enhanced sampling (TIES), and others.<sup>9,54,132,134,153,157,158</sup>

We recently introduced<sup>69</sup> an ACES method in AMBER that integrates the following novel features:

- Localized enhanced sampling states through tuning of intra- and intermolecular energy terms, e.g., noninteracting “dummy” states<sup>99</sup> with modified internal energy terms that eliminate kinetic traps;
- Robust alchemical transformation pathways to connect real and enhanced sampling states using new smoothstep softcore potentials, nonlinear Hamiltonian mixing, and flexible  $\lambda$ -scheduling capabilities;<sup>102</sup>

- Efficient Hamiltonian replica exchange MD (HREMD) frameworks that maintain equilibrium between  $\lambda$ -windows and enable enhanced sampling.

The ACES approach<sup>69</sup> has advantages due to its dual-topology nature<sup>159</sup> that allows it to overcome local “hot spot” problems encountered with REST/REST2.<sup>160</sup> As the ACES region of the  $\lambda = 0$  real state (e.g., Ligand 1) is being “annihilated” with respect to its interactions with the environment and transformation into an enhanced-sampled “dummy” state,<sup>99</sup> the ACES region of the  $\lambda = 1$  real state (e.g., Ligand 2) is being “created”. This concerted “counterdiffusion” of alchemical states produces minimal rearrangement of the environment along the  $\lambda$  path. Further, the computational overhead of the method is negligible relative to more conventional AFE simulations with HREMD. Although ACES can be used along with REST2-like methods added to further enhance sampling of the end states (which incurs added computational cost), results suggest that there is little gain beyond using ACES alone.<sup>69</sup>

Enhanced sampling methods such as ACES can reduce issues associated with ligands that exhibit multiple orientations or binding poses, especially when the free energy barriers between these conformational states are sufficiently low that interconversion is observed within the time scale of the simulations. On the other hand, if this cannot be achieved, then alternative strategies need to be pursued.<sup>70</sup> One straightforward, albeit time-consuming, way to deal with this situation is to calculate the free energy associated with each binding mode separately and use Boltzmann weighting to account for their collective free energy.<sup>161</sup> Emerging end-state alchemical reservoir methods will enable the precalculation of multiple ligand binding modes that can be integrated with existing enhanced sampling methods, such as ACES.

## 6. WHAT ARE SOME GENERAL RECOMMENDATIONS FOR PERFORMING AFE SIMULATIONS?

The following are some general recommendations for setting up and running simulations (further details are outlined in a recently reported workflow<sup>94</sup>):

- Carefully equilibrate each end state (node) prior to setting up an alchemical transformation (edge) simulation between the nodes. Use the same equilibrated structures of a given node consistently for any edge containing the node.
- Construct “dense” thermodynamic graphs that have sufficient redundancy to enable network-wide analysis<sup>34</sup> of cycle closure conditions and yield meaningful internal consistency checks.
- Use optimized alchemical transformation pathways, including smoothstep softcore potentials<sup>102</sup> and, if necessary, advanced  $\lambda$  scheduling features in order to maximize phase space overlap between windows.
- Apply robust enhanced sampling methods such as ACES<sup>69</sup> that leverage an HREMD framework to ensure that different  $\lambda$ -windows are kept in equilibrium.

Simulation results should be tested for convergence through block analysis, and statistical error estimates should be made<sup>1,33,34,162–164</sup> that include multiple independent trials of ACES runs. The next section discusses potential caveats and offers suggestions for analysis to help troubleshoot and improve the reliability of predicted results.

## 7. HOW DO I KNOW IF THERE ARE PROBLEMS WITH MY AFE CALCULATIONS?

AFE simulations, aside from issues associated with the accuracy of the force fields used, can encounter a number of caveats that limit their predictive capability. In what follows, we consider the most common use case in drug discovery: AFE simulations for a set of ligands arranged in a thermodynamic graph network, where the nodes in the graph represent real states and edges that connect nodes represent alchemical transformations between the real states. The real states thus form the “end states” (or “real-state end points”) for a given alchemical transformation. Within this context, the following are some guiding principles:

- Are the end-state (node) conformational ensembles and associated energy distributions correct and consistent within the network, i.e., are they the same for every connecting alchemical transformation (every edge containing the same node)?
- For a given alchemical transformation (edge), are the  $\lambda$ -window simulations sampling consistent conformational ensembles and energy distributions, i.e., are the  $\lambda$ -windows in equilibrium with one another?
- For the degree of sampling that is achieved, is the alchemical transformation pathway stable, i.e., do the  $\partial U/\partial \lambda$  distributions fluctuate stably (i.e., appear unimodal with small variance and show no signs of phase transition behavior in the  $\lambda$ -dimension) and is there sufficient phase space overlap between  $\lambda$ -windows to allow a reliable estimate of the free energy?

Of these guiding principles, often the most difficult one to correct is the first. In typical calculations, edges are computed in separate (independent) simulations, e.g., a HREMD simulation using ACES or the REST/REST2 method. For example, consider a particular node (“node 1”) that is connected to three other nodes (“nodes 2, 3, and 4”) in a thermodynamic graph, and let us label the edges connecting to node 1 as “edge (1–2), edge (1–3), and edge (1–4)”. Suppose that for each edge an HREMD simulation is performed such that the  $\lambda$ -windows, including the end states, are in equilibrium with one another. If simulations for each edge are performed separately, then it is not guaranteed (or even probable) that the end state distributions for node 1 derived independently from edge (1–2), edge (1–3), and edge (1–4) HREMD simulations will be statistically indistinguishable. In principle, one could set up a large network of HREMD simulations, where the edges are connected through a common node. This strategy imposes a constraint that the entire network of HREMD simulations be run in some way synchronously (even if exchanges are made asynchronously) and does not easily allow for the network to be extended to include new edges and nodes. An alternate strategy is to precompute the end state (node) distributions and store them as end-state alchemical reservoirs and then use them as ensemble baths for each node (i.e., have the reservoirs exchanging at the end state during an edge transformation so as to ensure a consistent end state distribution). A technical challenge arises as to how to rigorously map the set of noninteracting “dummy atoms” that are needed for an alchemical (edge) transformation onto a reservoir conformation where such dummy atoms are not present. These end-state reservoir methods are forthcoming and promise to considerably enhance the level of precision achievable in AFE simulations for drug discovery.

Once a strategy has been decided in terms of construction of a thermodynamic graph network, atom mapping procedure, and alchemical transformation pathway, the following are some valuable checks that can be performed:

- Perform comprehensive statistical error analysis<sup>1,33,34,162–164</sup> (of both correlated data samples and independent trials) such as block bootstrapping and forward/reverse sampling.
- Compare TI and MBAR free energy estimates for consistency within their estimated statistical errors.<sup>34</sup> If the variance between estimates is outside of reasonable error bounds, this is suggestive of problems that need to be addressed. Tracking how the MBAR result changes by progressively removing states in the analysis (approaching the BAR limit) could offer additional insight into the stability of the free energy estimate.
- Analyze the  $\langle \partial U / \partial \lambda \rangle_\lambda$  profiles as a function of  $\lambda$  and the variance at each  $\lambda$ -window. Windows that exhibit kinks and/or deviations from otherwise smooth profiles or that have anomalously large variances or bimodal  $\partial U / \partial \lambda$  distributions are likely problematic. A possible solution is to find a more suitable alchemical transformation pathway by considering alternative softcore potentials, atom mapping,  $\lambda$  scheduling (which may include sequential creation/annihilation of functional groups one at a time as opposed to all at once), or introduction of new chemical or alchemical intermediates (i.e., new nodes in the thermodynamic graph).
- Analyze phase space overlap, HREMD acceptance ratios, and round-trip statistics. Phase space overlap is typically correlated with the HREMD acceptance ratios and should never dip to values close to zero (values below 0.2 are of concern). HREMD simulations should see many walkers making “round trips” from one real state to the other and back again. Two common origins of poor phase space overlap are (1) the spacing between  $\lambda$  windows is too large and (2) first-order phase transitions in the  $\lambda$ -dimension can result in bimodal  $\partial U / \partial \lambda$  distributions. In the first case, a possible solution is to find more optimal  $\lambda$  spacing such that the phase space overlap is larger and more uniform, and if needed, increase the number of  $\lambda$ -windows appropriately. In the second case, it may be necessary to introduce new chemical or alchemical intermediates to further break up edges that exhibit these phase transitions.
- Analyze cycle closure conditions as independent consistency checks and perform Lagrange multiplier analysis to identify potentially problematic edges. If such an edge is identified, consider excluding it in the analysis (which might require adding a new edge to reconnect a node that was severed).

## 8. WHAT ARE SOME OTHER CONSIDERATIONS AND FUTURE DIRECTIONS?

There are a vast number of outstanding issues that are being actively addressed by a variety of groups at the forefront of the field. Some selected for mention here include the following:

- Methods to handle interfacial and buried (kinetically trapped) water molecules that can fluctuate in occupancy upon binding.<sup>83–85</sup>
- Charge-changing ligand perturbations and counterbalancing salt effects.<sup>165–169</sup>

- Alternative tautomers<sup>82,170</sup> and protonation states<sup>171</sup> of both ligand and target molecules.<sup>82,172,173</sup>
- Binding sites involving metal–ligand interactions.<sup>174,175</sup>
- Covalent inhibition.<sup>176,177</sup>

As the methods evolve to meet these and other challenges, it will become increasingly important to perform large-scale assessments<sup>178,179</sup> and conduct community-wide blind challenges.<sup>180,181</sup>

Emerging technologies that promise to improve the accuracy and precision of AFE calculations in drug discovery include the development of end-state ensemble reservoirs that can be used within networks to ensure consistent end states as well as continued evolution of sampling methods. Finally, there are a number of exciting advances in the development of new force fields that promise higher levels of accuracy, most notably classical polarizable force fields<sup>182–186</sup> and machine learning potentials (MLPs).<sup>187–190</sup> Of particular promise are the new methods that combine fast, approximate quantum-mechanical (QM) models with MLP corrections to achieve high accuracy (QM/ $\Delta$ -MLPs).<sup>173,191–196</sup> These methods are “universal” in the sense that unlike molecular mechanical force fields (including polarizable force fields), they do not assume a predetermined bonding topology and are able to accurately model different tautomers and protonation states. This is highly significant, as 30% of the compounds in vendor databases and 21% drug databases have potential tautomers<sup>197,198</sup> and it has been estimated that up to 95% of drug molecules contain ionizable groups.<sup>197</sup>

What is clear is that there is a driving need to continue to advance the state-of-the-art AFE simulations to improve both precision and accuracy to meet the evolving challenges in the design of new therapeutics. It is our hope that the current Perspective is useful in providing some insight into modern alchemical free energy methods and their role in drug discovery.

## AUTHOR INFORMATION

### Corresponding Author

Darrin M. York – Laboratory for Biomolecular Simulation Research, Institute for Quantitative Biomedicine, and Department of Chemistry and Chemical Biology, Rutgers University, Piscataway, New Jersey 08854, United States; [orcid.org/0000-0002-9193-7055](https://orcid.org/0000-0002-9193-7055); Email: [Darrin.York@rutgers.edu](mailto:Darrin.York@rutgers.edu)

Complete contact information is available at: <https://pubs.acs.org/10.1021/acsphyschemau.3c00033>

### Notes

The author declares no competing financial interest.

## ACKNOWLEDGMENTS

The author thanks Shi Zhang for assistance in assembling references and Yujun Tao for assistance with the graphical cover art. The author is grateful for the financial support provided by the National Institutes of Health (GM107485). Computational resources were provided by the Extreme Science and Engineering Discovery Environment (XSEDE), which is supported by National Science Foundation Grant ACI-1548562 (supercomputer Expanse at SDSC through allocation CHE190067), and by the Texas Advanced Computing Center (TACC) at the University of Texas at Austin (supercomputer Longhorn through allocation CHE20002).

## REFERENCES

- (1) *Free Energy Calculations: Theory and Applications in Chemistry and Biology*; Chipot, C., Pohorille, A., Eds.; Springer Series in Chemical Physics, Vol. 86; Springer: New York, 2007.
- (2) Roux, B. *Computational Modeling and Simulations of Biomolecular Systems*; World Scientific, 2021.
- (3) Jorgensen, W. L. Efficient drug lead discovery and optimization. *Acc. Chem. Res.* **2009**, *42*, 724–733.
- (4) Lee, T.-S.; Allen, B. K.; Giese, T. J.; Guo, Z.; Li, P.; Lin, C.; McGee, T. D., Jr.; Pearlman, D. A.; Radak, B. K.; Tao, Y.; Tsai, H.-C.; Xu, H.; Sherman, W.; York, D. M. Alchemical Binding Free Energy Calculations in AMBER20: Advances and Best Practices for Drug Discovery. *J. Chem. Inf. Model.* **2020**, *60*, 5595–5623.
- (5) Abel, R.; Wang, L.; Harder, E. D.; Berne, B. J.; Friesner, R. A. Advancing Drug Discovery through Enhanced Free Energy Calculations. *Acc. Chem. Res.* **2017**, *50*, 1625–1632.
- (6) Cournia, Z.; Allen, B. K.; Beuming, T.; Pearlman, D. A.; Radak, B. K.; Sherman, W. Rigorous Free Energy Simulations in Virtual Screening. *J. Chem. Inf. Model.* **2020**, *60*, 4153–4169.
- (7) Song, L. F.; Merz, K. M. Evolution of Alchemical Free Energy Methods in Drug Discovery. *J. Chem. Inf. Model.* **2020**, *60*, 5308–5318.
- (8) Mey, A. S. J. S.; Allen, B. K.; Bruce Macdonald, H. E.; Chodera, J. D.; Hahn, D. F.; Kuhn, M.; Michel, J.; Mobley, D. L.; Naden, L. N.; Prasad, S.; Rizzi, A.; Scheen, J.; Shirts, M. R.; Tresadern, G.; Xu, H. Best Practices for Alchemical Free Energy Calculations [Article v1.0]. *Living J. Comput. Mol. Sci.* **2020**, *2*, 18378.
- (9) Cournia, Z.; Chipot, C.; Roux, B.; York, D. M.; Sherman, W. Free Energy Methods in Drug Discovery—Introduction. In *Free Energy Methods in Drug Discovery: Current State and Future Directions*; Armacost, K. A., Thompson, D. C., Eds.; ACS Symposium Series 1397; American Chemical Society: Washington, DC, 2021; Chapter 1, pp 1–38.
- (10) Armacost, K. A.; Riniker, S.; Cournia, Z. Exploring Novel Directions in Free Energy Calculations. *J. Chem. Inf. Model.* **2020**, *60*, 5283–5286.
- (11) Lee, T.-S.; Cerutti, D. S.; Mermelstein, D.; Lin, C.; LeGrand, S.; Giese, T. J.; Roitberg, A.; Case, D. A.; Walker, R. C.; York, D. M. GPU-Accelerated Molecular Dynamics and Free Energy Methods in Amber18: Performance Enhancements and New Features. *J. Chem. Inf. Model.* **2018**, *58*, 2043–2050.
- (12) Lee, T.-S.; Tsai, H.-C.; Ganguly, A.; Giese, T. J.; York, D. M. Robust, Efficient and Automated Methods for Accurate Prediction of Protein-Ligand Binding Affinities in AMBER Drug Discovery Boost. In *Free Energy Methods in Drug Discovery: Current State and Future Directions*; Armacost, K. A., Thompson, D. C., Eds.; ACS Symposium Series 1397; American Chemical Society: Washington, DC, 2021; Chapter 7, pp 161–204.
- (13) McCammon, J. A.; Harvey, S. C. *Dynamics of Proteins and Nucleic Acids*; Cambridge University Press: Cambridge, U.K., 1987.
- (14) Brooks, C. L., III; Case, D. A. Theory and simulation. The control and timescale of structure and reactivity in biological systems: from peptide folding to cellular networks. *Curr. Opin. Struct. Biol.* **2003**, *13*, 143–145.
- (15) Garcia-Viloca, M.; Gao, J.; Karplus, M.; Truhlar, D. G. How enzymes work: Analysis by modern rate theory and computer simulations. *Science* **2004**, *303*, 186–195.
- (16) Ganguly, A.; Weissman, B. P.; Giese, T. J.; Li, N.-S.; Hoshika, S.; Rao, S.; Benner, S. A.; Piccirilli, J. A.; York, D. M. Confluence of theory and experiment reveals the catalytic mechanism of the Varkud satellite ribozyme. *Nat. Chem.* **2020**, *12*, 193–201.
- (17) Roux, B. Computational studies of the gramicidin channel. *Acc. Chem. Res.* **2002**, *35*, 366–375.
- (18) Dobson, C. M.; Karplus, M. The fundamentals of protein folding: bringing together theory and experiment. *Curr. Opin. Struct. Biol.* **1999**, *9*, 92–101.
- (19) Thirumalai, D.; Woodson, S. A. Kinetics of Folding of Proteins and RNA. *Acc. Chem. Res.* **1996**, *29*, 433–439.
- (20) Henriksen, N. M.; Fenley, A. T.; Gilson, M. K. Computational Calorimetry: High-Precision Calculation of Host-Guest Binding Thermodynamics. *J. Chem. Theory Comput.* **2015**, *11*, 4377–4394.
- (21) Gilson, M. K.; Zhou, H.-X. Calculation of protein-ligand binding affinities. *Annu. Rev. Biophys. Biomol. Struct.* **2007**, *36*, 21–42.
- (22) Deng, Y.; Roux, B. Computations of standard binding free energies with molecular dynamics simulations. *J. Phys. Chem. B* **2009**, *113*, 2234–2246.
- (23) Dixon, T.; Lotz, S. D.; Dickson, A. Predicting ligand binding affinity using on- and off-rates for the SAMPL6 SAMPLing challenge. *J. Comput.-Aided Mol. Des.* **2018**, *32*, 1001–1012.
- (24) Straatsma, T. P.; McCammon, J. A. Computational alchemy. *Annu. Rev. Phys. Chem.* **1992**, *43*, 407–435.
- (25) Sprik, M.; Ciccotti, G. Free energy from constrained molecular dynamics. *J. Chem. Phys.* **1998**, *109*, 7737–7744.
- (26) Trzesniak, D.; Kunz, A.-P. E.; van Gunsteren, W. F. A comparison of methods to compute the potential of mean force. *ChemPhysChem* **2007**, *8*, 162–169.
- (27) Kirkwood, J. G. Statistical mechanics of fluid mixtures. *J. Chem. Phys.* **1935**, *3*, 300–313.
- (28) Straatsma, T. P.; Berendsen, H. J. Free energy of ionic hydration: Analysis of a thermodynamic integration technique to evaluate free energy differences by molecular dynamics simulations. *J. Chem. Phys.* **1988**, *89*, 5876–5886.
- (29) Torrie, G. M.; Valleau, J. P. Nonphysical sampling distributions in Monte Carlo free-energy estimation: Umbrella sampling. *J. Comput. Phys.* **1977**, *23*, 187–199.
- (30) Tan, Z.; Gallicchio, E.; Lapelosa, M.; Levy, R. M. Theory of binless multi-state free energy estimation with applications to protein-ligand binding. *J. Chem. Phys.* **2012**, *136*, 144102.
- (31) Bennett, C. H. Efficient estimation of free energy differences from Monte Carlo data. *J. Comput. Phys.* **1976**, *22*, 245–268.
- (32) Shirts, M. R.; Pande, V. S. Comparison of efficiency and bias of free energies computed by exponential averaging, the Bennett acceptance ratio, and thermodynamic integration. *J. Chem. Phys.* **2005**, *122*, 144107.
- (33) Shirts, M. R.; Chodera, J. D. Statistically optimal analysis of samples from multiple equilibrium states. *J. Chem. Phys.* **2008**, *129*, 124105.
- (34) Giese, T. J.; York, D. M. Variational Method for Networkwide Analysis of Relative Ligand Binding Free Energies with Loop Closure and Experimental Constraints. *J. Chem. Theory Comput.* **2021**, *17*, 1326–1336.
- (35) Lee, T.-S.; Radak, B. K.; Pabis, A.; York, D. M. A new maximum likelihood approach for free energy profile construction from molecular simulations. *J. Chem. Theory Comput.* **2013**, *9*, 153–164.
- (36) Lee, T.-S.; Radak, B. K.; Huang, M.; Wong, K.-Y.; York, D. M. Roadmaps through free energy landscapes calculated using the multidimensional vFEP approach. *J. Chem. Theory Comput.* **2014**, *10*, 24–34.
- (37) Giese, T. J.; Ekesan, Ş.; York, D. M. Extension of the Variational Free Energy Profile and Multistate Bennett Acceptance Ratio Methods for High-Dimensional Potential of Mean Force Profile Analysis. *J. Phys. Chem. A* **2021**, *125*, 4216–4232.
- (38) Bonomi, M.; Branduardi, D.; Bussi, G.; Camilloni, C.; Provasi, D.; Raiteri, P.; Donadio, D.; Marinelli, F.; Pietrucci, F.; Broglia, R.; Parrinello, M. PLUMED: a portable plugin for free energy calculations with molecular dynamics. *Comput. Phys. Commun.* **2009**, *180*, 1961–1972.
- (39) Iannuzzi, M.; Laio, A.; Parrinello, M. Efficient exploration of reactive potential energy surfaces using car-parrinello molecular dynamics. *Phys. Rev. Lett.* **2003**, *90*, 238302.
- (40) Ensing, B.; De Vivo, M.; Liu, Z.; Moore, P.; Klein, M. L. Metadynamics as a tool for exploring free energy landscapes of chemical reactions. *Acc. Chem. Res.* **2006**, *39*, 73–81.
- (41) Kong, X.; Brooks, C. L., III  $\lambda$ -dynamics: A new approach to free energy calculations. *J. Chem. Phys.* **1996**, *105*, 2414–2423.
- (42) Raman, E. P.; Paul, T. J.; Hayes, R. L.; Brooks, C. L., 3rd Automated, Accurate, and Scalable Relative Protein–Ligand Binding

- Free-Energy Calculations Using Lambda Dynamics. *J. Chem. Theory Comput.* **2020**, *16*, 7895–7914.
- (43) Wouters, O. J.; McKee, M.; Luyten, J. Estimated Research and Development Investment Needed to Bring a New Medicine to Market, 2009–2018. *JAMA* **2020**, *323*, 844–853.
- (44) Chodera, J.; Mobley, D.; Shirts, M.; Dixon, R.; Branson, K.; Pande, V. Alchemical free energy methods for drug discovery: progress and challenges. *Curr. Opin. Struct. Biol.* **2011**, *21*, 150–160.
- (45) Mobley, D. L.; Klimovich, P. V. Perspective: Alchemical free energy calculations for drug discovery. *J. Chem. Phys.* **2012**, *137*, 230901.
- (46) Zwanzig, R. W. High-temperature equation of state by a perturbation method. I. Nonpolar gases. *J. Chem. Phys.* **1954**, *22*, 1420–1426.
- (47) Jarzynski, C. Nonequilibrium equality for free energy differences. *Phys. Rev. Lett.* **1997**, *78*, 2690–2693.
- (48) Crooks, G. E. Path-ensemble averages in systems driven far from equilibrium. *Phys. Rev. E* **2000**, *61*, 2361–2366.
- (49) Boresch, S.; Woodcock, H. L. Convergence of single-step free energy perturbation. *Mol. Phys.* **2017**, *115*, 1200–1213.
- (50) Gapsys, V.; Michielssens, S.; Peters, J. H.; de Groot, B. L.; Leonov, H. Calculation of binding free energies. *Methods Mol. Biol.* **2015**, *1215*, 173–209.
- (51) Jeong, D.; Andricioaei, I. Reconstructing equilibrium entropy and enthalpy profiles from non-equilibrium pulling. *J. Chem. Phys.* **2013**, *138*, 114110.
- (52) Wei, D.; Song, Y.; Wang, F. A simple molecular mechanics potential for  $\mu\text{m}$  scale graphene simulations from the adaptive force matching method. *J. Chem. Phys.* **2011**, *134*, 184704.
- (53) Kearns, F. L.; Hudson, P. S.; Woodcock, H. L.; Boresch, S. Computing converged free energy differences between levels of theory via nonequilibrium work methods: Challenges and opportunities. *J. Comput. Chem.* **2017**, *38*, 1376–1388.
- (54) Suh, D.; Radak, B. K.; Chipot, C.; Roux, B. Enhanced configurational sampling with hybrid non-equilibrium molecular dynamics-Monte Carlo propagator. *J. Chem. Phys.* **2018**, *148*, 014101.
- (55) Kofke, D. A.; Cummings, P. T. Quantitative comparison and optimization of methods for evaluating the chemical potential by molecular simulation. *Mol. Phys.* **1997**, *92*, 973–996.
- (56) Wu, D.; Kofke, D. A. Phase-space overlap measures. II. Design and implementation of staging methods for free-energy calculations. *J. Chem. Phys.* **2005**, *123*, 084109.
- (57) Kofke, D. A. On the sampling requirements for exponential-work free-energy calculations. *Mol. Phys.* **2006**, *104*, 3701–3708.
- (58) Giese, T. J.; York, D. M. Development of a Robust Indirect Approach for MM  $\rightarrow$  QM Free Energy Calculations That Combines Force-Matched Reference Potential and Bennett's Acceptance Ratio Methods. *J. Chem. Theory Comput.* **2019**, *15*, 5543–5562.
- (59) Genheden, S.; Ryde, U. The MM/PBSA and MM/GBSA methods to estimate ligand-binding affinities. *Expert Opin. Drug Discovery* **2015**, *10*, 449–461.
- (60) Åqvist, J.; Luzhkov, V. B.; Brandsdal, B. O. Ligand binding affinities from MD simulations. *Acc. Chem. Res.* **2002**, *35*, 358–365.
- (61) Bruckner, S.; Boresch, S. Efficiency of alchemical free energy simulations. II. Improvements for thermodynamic integration. *J. Comput. Chem.* **2011**, *32*, 1320–1333.
- (62) Shyu, C.; Ytreberg, F. M. Accurate estimation of solvation free energy using polynomial fitting techniques. *J. Comput. Chem.* **2011**, *32*, 134–141.
- (63) Hudson, P. S.; Woodcock, H. L.; Boresch, S. Use of Nonequilibrium Work Methods to Compute Free Energy Differences Between Molecular Mechanical and Quantum Mechanical Representations of Molecular Systems. *J. Phys. Chem. Lett.* **2015**, *6*, 4850–4856.
- (64) Kearns, F. L.; Hudson, P. S.; Boresch, S.; Woodcock, H. L. Methods for Efficiently and Accurately Computing Quantum Mechanical Free Energies for Enzyme Catalysis. *Methods Enzymol.* **2016**, *577*, 75–104.
- (65) Schöller, A.; Kearns, F.; Woodcock, H. L.; Boresch, S. Optimizing the Calculation of Free Energy Differences in Nonequilibrium Work SQM/MM Switching Simulations. *J. Phys. Chem. B* **2022**, *126*, 2798–2811.
- (66) Ruiter, A. d.; Oostenbrink, C. Extended Thermodynamic Integration: Efficient Prediction of Lambda Derivatives at Non-simulated Points. *J. Chem. Theory Comput.* **2016**, *12*, 4476–4486.
- (67) Hummer, G.; Szabo, A. Free Energy Surfaces from Single-Molecule Force Spectroscopy. *Acc. Chem. Res.* **2005**, *38*, 504–513.
- (68) Gapsys, V.; Pérez-Benito, L.; Aldeghi, M.; Seeliger, D.; van Vlijmen, H.; Tresadern, G.; de Groot, B. L. Large scale relative protein ligand binding affinities using non-equilibrium alchemy. *Chem. Sci.* **2020**, *11*, 1140–1152.
- (69) Lee, T.-S.; Tsai, H.-C.; Ganguly, A.; York, D. M. ACES: Optimized Alchemically Enhanced Sampling. *J. Chem. Theory Comput.* **2023**, *19*, 472–487.
- (70) Cournia, Z.; Allen, B.; Sherman, W. Relative Binding Free Energy Calculations in Drug Discovery: Recent Advances and Practical Considerations. *J. Chem. Inf. Model.* **2017**, *57*, 2911–2937.
- (71) Athanasiou, C.; Vasilakaki, S.; Dellis, D.; Cournia, Z. Using physics-based pose predictions and free energy perturbation calculations to predict binding poses and relative binding affinities for FXR ligands in the D3R Grand Challenge 2. *J. Comput.-Aided Mol. Des.* **2018**, *32*, 21–44.
- (72) Schneidman-Duhovny, D.; Pellarin, R.; Sali, A. Uncertainty in integrative structural modeling. *Curr. Opin. Struct. Biol.* **2014**, *28*, 96–104.
- (73) Webb, B.; Sali, A. Protein Structure Modeling with MODELLER. *Methods Mol. Biol.* **2021**, 2199, 239–255.
- (74) Rout, M. P.; Sali, A. Principles for Integrative Structural Biology Studies. *Cell* **2019**, *177*, 1384–1403.
- (75) Baek, M.; et al. Accurate prediction of protein structures and interactions using a three-track neural network. *Science* **2021**, *373*, 871–876.
- (76) Jumper, J.; et al. Highly accurate protein structure prediction with AlphaFold. *Nature* **2021**, *596*, 583–589.
- (77) Wong, F.; Krishnan, A.; Zheng, E. J.; Stärk, H.; Manson, A. L.; Earl, A. M.; Jaakkola, T.; Collins, J. J. Benchmarking AlphaFold-enabled molecular docking predictions for antibiotic discovery. *Mol. Syst. Biol.* **2022**, *18*, No. e11081.
- (78) Crampon, K.; Giorkallos, A.; Deldossi, M.; Baud, S.; Steffanel, L. A. Machine-learning methods for ligand–protein molecular docking. *Drug Discovery Today* **2022**, *27*, 151–164.
- (79) Gentile, F.; Yaacoub, J. C.; Gleave, J.; Fernandez, M.; Ton, A.-T.; Ban, F.; Stern, A.; Cherkasov, A. Artificial intelligence-enabled virtual screening of ultra-large chemical libraries with deep docking. *Nat. Protoc.* **2022**, *17*, 672–697.
- (80) Liu, Y.; Yang, X.; Gan, J.; Chen, S.; Xiao, Z.-X.; Cao, Y. CB-Dock2: improved protein–ligand blind docking by integrating cavity detection, docking and homologous template fitting. *Nucleic Acids Res.* **2022**, *50*, W159–W164.
- (81) Sadybekov, A. A.; et al. Synthon-based ligand discovery in virtual libraries of over 11 billion compounds. *Nature* **2022**, *601*, 452–459.
- (82) Hu, Y.; Sherborne, B.; Lee, T.-S.; Case, D. A.; York, D. M.; Guo, Z. The importance of protonation and tautomerization in relative binding affinity prediction: a comparison of AMBER TI and Schrödinger FEP. *J. Comput.-Aided Mol. Des.* **2016**, *30*, 533–539.
- (83) Schiebel, J.; Gaspari, R.; Wulsdorf, T.; Ngo, K.; Sohn, C.; Schrader, T. E.; Cavalli, A.; Ostermann, A.; Heine, A.; Klebe, G. Intriguing role of water in protein–ligand binding studied by neutron crystallography on trypsin complexes. *Nat. Commun.* **2018**, *9*, 3559.
- (84) Ben-Shalom, I. Y.; Lin, C.; Kurtzman, T.; Walker, R. C.; Gilson, M. K. Simulating Water Exchange to Buried Binding Sites. *J. Chem. Theory Comput.* **2019**, *15*, 2684–2691.
- (85) Ben-Shalom, I. Y.; Lin, Z.; Radak, B. K.; Lin, C.; Sherman, W.; Gilson, M. K. Accounting for the Central Role of Interfacial Water in Protein–Ligand Binding Free Energy Calculations. *J. Chem. Theory Comput.* **2020**, *16*, 7883–7894.
- (86) Giambaşu, G. M.; Case, D. A.; York, D. M. Predicting Site-Binding Modes of Ions and Water to Nucleic Acids Using Molecular Solvation Theory. *J. Am. Chem. Soc.* **2019**, *141*, 2435–2445.

- (87) Giambaşu, G. M.; Luchko, T.; Herschlag, D.; York, D. M.; Case, D. A. Ion counting from explicit-solvent simulations and 3D-RISM. *Biophys. J.* **2014**, *106*, 883–894.
- (88) Giambaşu, G. M.; Gebala, M. K.; Panteva, M. T.; Luchko, T.; Case, D. A.; York, D. M. Competitive Interaction of Monovalent Cations With DNA From 3D-RISM. *Nucleic Acids Res.* **2015**, *43*, 8405–8415.
- (89) Ioannidis, H.; Drakopoulos, A.; Tzitzoglaki, C.; Homeyer, N.; Kolarov, F.; Gkeka, P.; Freudenberger, K.; Liolios, C.; Gauglitz, G.; Cournia, Z.; Gohlke, H.; Kolocouris, A. Alchemical Free Energy Calculations and Isothermal Titration Calorimetry Measurements of Aminoadamantanes Bound to the Closed State of Influenza A/M2TM. *J. Chem. Inf. Model.* **2016**, *56*, 862–76.
- (90) Negami, T.; Araki, M.; Okuno, Y.; Terada, T. Calculation of absolute binding free energies between the hERG channel and structurally diverse drugs. *Sci. Rep.* **2019**, *9*, 16586.
- (91) Katz, D.; Sindhikara, D.; DiMattia, M.; Leffler, A. E. Potency-Enhancing Mutations of Gating Modifier Toxins for the Voltage-Gated Sodium Channel NaV1.7 Can Be Predicted Using Accurate Free-Energy Calculations. *Toxins* **2021**, *13*, 193.
- (92) Pitman, M.; Hahn, D. F.; Tresadern, G.; Mobley, D. L. To Design Scalable Free Energy Perturbation Networks, Optimal Is Not Enough. *J. Chem. Inf. Model.* **2023**, *63*, 1776–1793.
- (93) Liu, S.; Wu, Y.; Lin, T.; Abel, R.; Redmann, J. P.; Summa, C. M.; Jaber, V. R.; Lim, N. M.; Mobley, D. L. Lead optimization mapper: automating free energy calculations for lead optimization. *J. Comput.-Aided Mol. Des.* **2013**, *27*, 755–770.
- (94) Ganguly, A.; Tsai, H.-C.; Fernández-Pendás, M.; Lee, T.-S.; Giese, T. J.; York, D. M. AMBER Drug Discovery Boost Tools: Automated Workflow for Production Free-Energy Simulation Setup and Analysis (ProFESSA). *J. Chem. Inf. Model.* **2022**, *62*, 6069–6083.
- (95) Xu, H. Optimal Measurement Network of Pairwise Differences. *J. Chem. Inf. Model.* **2019**, *59*, 4720–4728.
- (96) Li, P.; Li, Z.; Wang, Y.; Dou, H.; Radak, B. K.; Allen, B. K.; Sherman, W.; Xu, H. Precise Binding Free Energy Calculations for Multiple Molecules Using an Optimal Measurement Network of Pairwise Differences. *J. Chem. Theory Comput.* **2022**, *18*, 650–663.
- (97) S., S.; Roux, B.; Andersen, O. S. Free Energy Simulations: Thermodynamic Reversibility and Variability. *J. Phys. Chem. B* **2000**, *104*, 5179–5190.
- (98) Boresch, S. The Role of Bonded Energy Terms in Free Energy Simulations - Insights from Analytical Results. *Mol. Simul.* **2002**, *28*, 13–37.
- (99) Fleck, M.; Wieder, M.; Boresch, S. Dummy Atoms in Alchemical Free Energy Calculations. *J. Chem. Theory Comput.* **2021**, *17*, 4403–4419.
- (100) Boresch, S.; Tettinger, F.; Leitgeb, M.; Karplus, M. Absolute binding free energies: a quantitative approach for their calculation. *J. Phys. Chem. B* **2003**, *107*, 9535–9551.
- (101) Wang, J.; Deng, Y.; Roux, B. Absolute binding free energy calculations using molecular dynamics simulations with restraining potentials. *Biophys. J.* **2006**, *91*, 2798–2814.
- (102) Tsai, H.-C.; Lee, T.-S.; Ganguly, A.; Giese, T. J.; Ebert, M. C.; Labute, P.; Merz, K. M., Jr; York, D. M. AMBER Free Energy Tools: A New Framework for the Design of Optimized Alchemical Transformation Pathways. *J. Chem. Theory Comput.* **2023**, *19*, 640–658.
- (103) Baumann, H. M.; Dybeck, E.; McClendon, C. L.; Pickard, F. C., 4th; Gapsys, V.; Pérez-Benito, L.; Hahn, D. F.; Tresadern, G.; Mathiowetz, A. M.; Mobley, D. L. Broadening the Scope of Binding Free Energy Calculations Using a Separated Topologies Approach. *J. Chem. Theory Comput.* **2023**, *19*, 5058–5076.
- (104) Azimi, S.; Wu, J. Z.; Khuttan, S.; Kurtzman, T.; Deng, N.; Gallicchio, E. Application of the alchemical transfer and potential of mean force methods to the SAMPL8 host-guest blinded challenge. *J. Comput.-Aided Mol. Des.* **2022**, *36*, 63–76.
- (105) Azimi, S.; Khuttan, S.; Wu, J. Z.; Pal, R. K.; Gallicchio, E. Relative Binding Free Energy Calculations for Ligands with Diverse Scaffolds with the Alchemical Transfer Method. *J. Chem. Inf. Model.* **2022**, *62*, 309–323.
- (106) Sabanés Zariquiey, F.; Pérez, A.; Majewski, M.; Gallicchio, E.; De Fabritiis, G. Validation of the Alchemical Transfer Method for the Estimation of Relative Binding Affinities of Molecular Series. *J. Chem. Inf. Model.* **2023**, *63*, 2438–2444.
- (107) de Ruiter, A.; Petrov, D.; Oostenbrink, C. Optimization of Alchemical Pathways Using Extended Thermodynamic Integration. *J. Chem. Theory Comput.* **2021**, *17*, 56–65.
- (108) König, G.; Brooks, B. R.; Thiel, W.; York, D. M. On the convergence of multi-scale free energy simulations. *Mol. Simul.* **2018**, *44*, 1062–1081.
- (109) Wu, D.; Kofke, D. A. Phase-space overlap measures. I. Fail-safe bias detection in free energies calculated by molecular simulation. *J. Chem. Phys.* **2005**, *123*, 054103.
- (110) Beutler, T. C.; Mark, A. E.; van Schaik, R. C.; Gerber, P. R.; van Gunsteren, W. F. Avoiding singularities and numerical instabilities in free energy calculations based on molecular simulations. *Chem. Phys. Lett.* **1994**, *222*, 529–539.
- (111) Steinbrecher, T.; Joung, I.; Case, D. A. Soft-Core Potentials in Thermodynamic Integration: Comparing One- and Two-Step Transformations. *J. Comput. Chem.* **2011**, *32*, 3253–3263.
- (112) Hornak, V.; Simmerling, C. Development of softcore potential functions for overcoming steric barriers in molecular dynamics simulations. *J. Mol. Graphics Model.* **2004**, *22*, 405–413.
- (113) Giese, T. J.; York, D. M. A GPU-Accelerated Parameter Interpolation Thermodynamic Integration Free Energy Method. *J. Chem. Theory Comput.* **2018**, *14*, 1564–1582.
- (114) Gapsys, V.; Seeliger, D.; de Groot, B. L. New Soft-Core Potential Function for Molecular Dynamics Based Alchemical Free Energy Calculations. *J. Chem. Theory Comput.* **2012**, *8*, 2373–2382.
- (115) Buelens, F. P.; Grubmüller, H. Linear-scaling soft-core scheme for alchemical free energy calculations. *J. Comput. Chem.* **2012**, *33*, 25–33.
- (116) Pal, R. K.; Gallicchio, E. Perturbation potentials to overcome order/disorder transitions in alchemical binding free energy calculations. *J. Chem. Phys.* **2019**, *151*, 124116.
- (117) Mezei, M. Polynomial path for the calculation of liquid state free energies from computer simulations tested on liquid water. *J. Comput. Chem.* **1992**, *13*, 651–656.
- (118) Resat, H.; Mezei, M. Studies on free energy calculations. I. Thermodynamic integration using a polynomial path. *J. Chem. Phys.* **1993**, *99*, 6052–6061.
- (119) Simonson, T. Free energy of particle insertion. *Mol. Phys.* **1993**, *80*, 441–447.
- (120) Steinbrecher, T.; Mobley, D. L.; Case, D. A. Nonlinear scaling schemes for Lennard-Jones interactions in free energy calculations. *J. Chem. Phys.* **2007**, *127*, 214108.
- (121) Jiang, W.; Chipot, C.; Roux, B. Computing Relative Binding Affinity of Ligands to Receptor: An Effective Hybrid Single-Dual-Topology Free-Energy Perturbation Approach in NAMD. *J. Chem. Inf. Model.* **2019**, *59*, 3794–3802.
- (122) König, G.; Glaser, N.; Schroeder, B.; Kubincová, A.; Hünenberger, P. H.; Riniker, S. An Alternative to Conventional  $\lambda$ -Intermediate States in Alchemical Free Energy Calculations:  $\lambda$ -Enveloping Distribution Sampling. *J. Chem. Inf. Model.* **2020**, *60*, 5407–5423.
- (123) König, G.; Ries, B.; Hünenberger, P. H.; Riniker, S. Efficient Alchemical Intermediate States in Free Energy Calculations Using  $\lambda$ -Enveloping Distribution Sampling. *J. Chem. Theory Comput.* **2021**, *17*, 5805–5815.
- (124) Reinhardt, M.; Grubmüller, H. Determining Free-Energy Differences Through Variationally Derived Intermediates. *J. Chem. Theory Comput.* **2020**, *16*, 3504–3512.
- (125) Blondel, A. Ensemble Variance in Free Energy Calculations by Thermodynamic Integration: Theory, Optimal “Alchemical” Path, and Practical Solutions. *J. Comput. Chem.* **2004**, *25*, 985–993.
- (126) Pham, T. T.; Shirts, M. R. Optimal pairwise and non-pairwise alchemical pathways for free energy calculations of molecular transformation in solution phase. *J. Chem. Phys.* **2012**, *136*, 124120.

- (127) Tsai, H.-C.; Tao, Y.; Lee, T.-S.; Merz, K. M.; York, D. M. Validation of Free Energy Methods in AMBER. *J. Chem. Inf. Model.* **2020**, *60*, 5296–5300.
- (128) Lee, T.-S.; Lin, Z.; Allen, B. K.; Lin, C.; Radak, B. K.; Tao, Y.; Tsai, H.-C.; Sherman, W.; York, D. M. Improved Alchemical Free Energy Calculations with Optimized Smoothstep Softcore Potentials. *J. Chem. Theory Comput.* **2020**, *16*, 5512–5525.
- (129) Fajer, M.; Hamelberg, D.; McCammon, J. A. Replica-Exchange Accelerated Molecular Dynamics (REXAMD) Applied to Thermodynamic Integration. *J. Chem. Theory Comput.* **2008**, *4*, 1565–1569.
- (130) Zwier, M. C.; Chong, L. T. Reaching biological timescales with all-atom molecular dynamics simulations. *Curr. Opin. Pharmacol.* **2010**, *10*, 745–752.
- (131) Gallicchio, E.; Levy, R. M. Advances in all atom sampling methods for modeling protein-ligand binding affinities. *Curr. Opin. Struct. Biol.* **2011**, *21*, 161–166.
- (132) Mitsutake, A.; Mori, Y.; Okamoto, Y. Enhanced sampling algorithms. *Methods Mol. Biol.* **2013**, *924*, 153–195.
- (133) Bernardi, R. C.; Melo, M. C. R.; Schulten, K. Enhanced sampling techniques in molecular dynamics simulations of biological systems. *Biochim. Biophys. Acta* **2015**, *1850*, 872–877.
- (134) Yang, Y. I.; Shao, Q.; Zhang, J.; Yang, L.; Gao, Y. Q. Enhanced sampling in molecular dynamics. *J. Chem. Phys.* **2019**, *151*, No. 070902.
- (135) Invernizzi, M.; Piaggi, P. M.; Parrinello, M. Unified Approach to Enhanced Sampling. *Phys. Rev. X* **2020**, *10*, No. 041034.
- (136) Hénin, J.; Lelièvre, T.; Shirts, M. R.; Valsson, O.; Delemotte, L. Enhanced Sampling Methods for Molecular Dynamics Simulations [Article v1.0]. *Living J. Comput. Mol. Sci.* **2022**, *4*, 1583.
- (137) Kamenik, A. S.; Linker, S. M.; Riniker, S. Enhanced sampling without borders: on global biasing functions and how to reweight them. *Phys. Chem. Chem. Phys.* **2022**, *24*, 1225–1236.
- (138) Lelièvre, T.; Rousset, M.; Stoltz, G. *Free Energy Computations*; Imperial College Press, 2010.
- (139) Cuendet, M. A.; Tuckerman, M. E. Alchemical Free Energy Differences in Flexible Molecules from Thermodynamic Integration or Free Energy Perturbation Combined with Driven Adiabatic Dynamics. *J. Chem. Theory Comput.* **2012**, *8*, 3504–3512.
- (140) Wan, S.; Tresadern, G.; Pérez-Benito, L.; van Vlijmen, H.; Covey, P. V. Accuracy and Precision of Alchemical Relative Free Energy Predictions with and without Replica-Exchange. *Adv. Theory Simul.* **2020**, *3*, 1900195.
- (141) Sugita, Y.; Okamoto, Y. Replica-exchange molecular dynamics method for protein folding. *Chem. Phys. Lett.* **1999**, *314*, 141–151.
- (142) Sugita, Y.; Okamoto, Y. Replica-exchange multicanonical algorithm and multicanonical replica-exchange method for simulating systems with rough energy landscape. *Chem. Phys. Lett.* **2000**, *329*, 261–270.
- (143) Zhou, R.; Berne, B. J. Can a continuum solvent model reproduce the free energy landscape of a  $\beta$ -hairpin folding in water? *Proc. Natl. Acad. Sci. U.S.A.* **2002**, *99*, 12777–12782.
- (144) Comer, J.; Phillips, J. C.; Schulten, K.; Chipot, C. Multiple-Replica Strategies for Free-Energy Calculations in NAMD: Multiple-Walker Adaptive Biasing Force and Walker Selection Rules. *J. Chem. Theory Comput.* **2014**, *10*, 5276–5285.
- (145) Souaille, M.; Roux, B. Extension to the weighted histogram analysis method: Combining umbrella sampling with free energy calculations. *Comput. Phys. Commun.* **2001**, *135*, 40–57.
- (146) Marinari, E.; Parisi, G. Simulated Tempering: A New Monte Carlo Scheme. *Europhys. Lett.* **1992**, *19*, 451–458.
- (147) Hansmann, U. H. E. Parallel tempering algorithm for conformational studies of biological molecules. *Chem. Phys. Lett.* **1997**, *281*, 140–150.
- (148) Laio, A.; Parrinello, M. Escaping free-energy minima. *Proc. Natl. Acad. Sci. U.S.A.* **2002**, *99*, 12562–12566.
- (149) Wu, X.; Brooks, B. R. Self-guided molecular dynamics simulation based on concerted movement. *Biophys. J.* **2023**, *122*, 420A.
- (150) Liu, P.; Kim, B.; Friesner, R. A.; Berne, B. J. Replica exchange with solute tempering: A method for sampling biological systems in explicit water. *Proc. Natl. Acad. Sci. U.S.A.* **2005**, *102*, 13749–13754.
- (151) Wang, L.; Friesner, R. A.; Berne, B. Replica Exchange with Solute Scaling: A More Efficient Version of Replica Exchange with Solute Tempering (REST2). *J. Phys. Chem. B* **2011**, *115*, 9431–9438.
- (152) Berg, B. A.; Neuhaus, T. Multicanonical ensemble: A new approach to simulate first-order phase transitions. *Phys. Rev. Lett.* **1992**, *68*, 9–12.
- (153) Mitsutake, A.; Sugita, Y.; Okamoto, Y. Generalized-ensemble algorithms for molecular simulations of biopolymers. *Biopolymers* **2001**, *60*, 96–123.
- (154) Mitsutake, A.; Sugita, Y.; Okamoto, Y. Replica-exchange multicanonical and multicanonical replica-exchange Monte Carlo simulations of peptides. I. Formulation and benchmark test. *J. Chem. Phys.* **2003**, *118*, 6664–6675.
- (155) Zheng, L.; Chen, M.; Yang, W. Random walk in orthogonal space to achieve efficient free-energy simulation of complex systems. *Proc. Natl. Acad. Sci. U.S.A.* **2008**, *105*, 20227–20232.
- (156) Perthold, J. W.; Petrov, D.; Oostenbrink, C. Toward Automated Free Energy Calculation with Accelerated Enveloping Distribution Sampling (A-EDS). *J. Chem. Inf. Model.* **2020**, *60*, 5395–5406.
- (157) Bieler, N. S.; Hünenberger, P. H. Orthogonal sampling in free-energy calculations of residue mutations in a tripeptide: TI versus  $\lambda$ -LEUS. *J. Comput. Chem.* **2015**, *36*, 1686–1697.
- (158) Okamoto, Y. Generalized-ensemble algorithms: enhanced sampling techniques for Monte Carlo and molecular dynamics simulations. *J. Mol. Graphics Model.* **2004**, *22*, 425–439.
- (159) Min, D.; Li, H.; Li, G.; Bitetti-Putzer, R.; Yang, W. Synergistic approach to improve “alchemical” free energy calculation in rugged energy surface. *J. Chem. Phys.* **2007**, *126*, 144109.
- (160) Kamiya, M.; Sugita, Y. Flexible selection of the solute region in replica exchange with solute tempering: Application to protein-folding simulations. *J. Chem. Phys.* **2018**, *149*, 072304.
- (161) Kaus, J. W.; Harder, E.; Lin, T.; Abel, R.; McCammon, J. A.; Wang, L. How to deal with multiple binding poses in alchemical relative protein-ligand binding free energy calculations. *J. Chem. Theory Comput.* **2015**, *11*, 2670–2679.
- (162) Chipot, C.; Rozanska, X.; Dixit, S. B. Can free energy calculations be fast and accurate at the same time? Binding of low-affinity, non-peptide inhibitors to the SH2 domain of the src protein. *J. Comput.-Aided Mol. Des.* **2005**, *19*, 765–770.
- (163) Paliwal, H.; Shirts, M. R. A benchmark test set for alchemical free energy transformations and its use to quantify error in common free energy methods. *J. Chem. Theory Comput.* **2011**, *7*, 4115–4134.
- (164) Klimovich, P. V.; Shirts, M. R.; Mobley, D. L. Guidelines for the analysis of free energy calculations. *J. Comput.-Aided Mol. Des.* **2015**, *29*, 397–411.
- (165) Gao, K.; Yin, J.; Henriksen, N. M.; Fenley, A. T.; Gilson, M. K. Binding Enthalpy Calculations for a Neutral Host-Guest Pair Yield Widely Divergent Salt Effects across Water Models. *J. Chem. Theory Comput.* **2015**, *11*, 4555–4564.
- (166) Chen, W.; Deng, Y.; Russell, E.; Wu, Y.; Abel, R.; Wang, L. Accurate Calculation of Relative Binding Free Energies between Ligands with Different Net Charges. *J. Chem. Theory Comput.* **2018**, *14*, 6346–6358.
- (167) Clark, A. J.; Negron, C.; Hauser, K.; Sun, M.; Wang, L.; Abel, R.; Friesner, R. A. Relative Binding Affinity Prediction of Charge-Changing Sequence Mutations with FEP in Protein–Protein Interfaces. *J. Mol. Biol.* **2019**, *431*, 1481–1493.
- (168) Öhlknecht, C.; Perthold, J. W.; Lier, B.; Oostenbrink, C. Charge-Changing Perturbations and Path Sampling via Classical Molecular Dynamic Simulations of Simple Guest–Host Systems. *J. Chem. Theory Comput.* **2020**, *16*, 7721–7734.
- (169) Wu, Z.; Biggin, P. C. Correction Schemes for Absolute Binding Free Energies Involving Lipid Bilayers. *J. Chem. Theory Comput.* **2022**, *18*, 2657–2672.
- (170) Bharatam, P. V.; Valanju, O. R.; Wani, A. A.; Dhaked, D. K. Importance of tautomerism in drugs. *Drug Discovery Today* **2023**, *28*, 103494.
- (171) Swails, J. M.; York, D. M.; Roitberg, A. E. Constant pH replica exchange molecular dynamics in explicit solvent using discrete

- protonation states: Implementation, testing, and validation. *J. Chem. Theory Comput.* **2014**, *10*, 1341–1352.
- (172) de Oliveira, C.; Yu, H. S.; Chen, W.; Abel, R.; Wang, L. Rigorous Free Energy Perturbation Approach to Estimating Relative Binding Affinities between Ligands with Multiple Protonation and Tautomeric States. *J. Chem. Theory Comput.* **2019**, *15*, 424–435.
- (173) Zeng, J.; Tao, Y.; Giese, T. J.; York, D. M. Modern semiempirical electronic structure methods and machine learning potentials for drug discovery: Conformers, tautomers, and protonation states. *J. Chem. Phys.* **2023**, *158*, 124110.
- (174) Riccardi, L.; Genna, V.; De Vivo, M. Metal-ligand interactions in drug design. *Nat. Rev. Chem.* **2018**, *2*, 100–112.
- (175) Palermo, G.; Spinello, A.; Saha, A.; Magistrato, A. Frontiers of metal-coordinating drug design. *Expert Opin. Drug Discovery* **2021**, *16*, 497–511.
- (176) Baillie, T. A. Targeted Covalent Inhibitors for Drug Design. *Angew. Chem., Int. Ed.* **2016**, *55*, 13408–13421.
- (177) Chan, A. H.; Lee, W.-G.; Spasov, K. A.; Cisneros, J. A.; Kudalkar, S. N.; Petrova, Z. O.; Buckingham, A. B.; Anderson, K. S.; Jorgensen, W. L. Covalent inhibitors for eradication of drug-resistant HIV-1 reverse transcriptase: From design to protein crystallography. *Proc. Natl. Acad. Sci. U.S.A.* **2017**, *114*, 9725–9730.
- (178) Abel, R.; Wang, L.; Mobley, D. L.; Friesner, R. A. A Critical Review of Validation, Blind Testing, and Real-World Use of Alchemical Protein-Ligand Binding Free Energy Calculations. *Curr. Top. Med. Chem.* **2017**, *17*, 2577–2585.
- (179) Schindler, C. E. M.; et al. Large-Scale Assessment of Binding Free Energy Calculations in Active Drug Discovery Projects. *J. Chem. Inf. Model.* **2020**, *60*, 5457–5474.
- (180) Amezcua, M.; El Khoury, L.; Mobley, D. L. SAMPL7 Host–Guest Challenge Overview: assessing the reliability of polarizable and non-polarizable methods for binding free energy calculations. *J. Comput.-Aided Mol. Des.* **2021**, *35*, 1–35.
- (181) Tielker, N.; Eberlein, L.; Beckstein, O.; Güssregen, S.; Iorga, B. I.; Kast, S. M.; Liu, S. Perspective on the SAMPL and D3R Blind Prediction Challenges for Physics-Based Free Energy Methods. In *Free Energy Methods in Drug Discovery: Current State and Future Directions*; Armacost, K. A., Thompson, D. C., Eds.; ACS Symposium Series 1397; American Chemical Society: Washington, DC, 2021; Chapter 3, pp 67–107.
- (182) Ren, P.; Wu, C.; Ponder, J. W. Polarizable Atomic Multipole-Based Molecular Mechanics for Organic Molecules. *J. Chem. Theory Comput.* **2011**, *7*, 3143–3161.
- (183) Zhang, C.; Lu, C.; Jing, Z.; Wu, C.; Piquemal, J. P.; Ponder, J. W.; Ren, P. Amoeba Polarizable Atomic Multipole Force Field for Nucleic Acids. *J. Chem. Theory Comput.* **2018**, *14*, 2084–2108.
- (184) Shi, Y.; Laury, M. L.; Wang, Z.; Ponder, J. W. AMOEBA binding free energies for the SAMPL7 TrimerTrip host–guest challenge. *J. Comput.-Aided Mol. Des.* **2021**, *35*, 79–93.
- (185) Lemkul, J. A.; Huang, J.; Roux, B.; MacKerell, A. D., Jr. An Empirical Polarizable Force Field Based on the Classical Drude Oscillator Model: Development History and Recent Applications. *Chem. Rev.* **2016**, *116*, 4983–5013.
- (186) Lemkul, J. A.; MacKerell, A. D., Jr. Polarizable Force Field for DNA Based on the Classical Drude Oscillator: II. Microsecond Molecular Dynamics Simulations of Duplex DNA. *J. Chem. Theory Comput.* **2017**, *13*, 2072–2085.
- (187) Smith, J. S.; Isayev, O.; Roitberg, A. E. ANI-1: an extensible neural network potential with DFT accuracy at force field computational cost. *Chem. Sci.* **2017**, *8*, 3192–3203.
- (188) Smith, J. S.; Nebgen, B.; Lubbers, N.; Isayev, O.; Roitberg, A. E. Less is more: Sampling chemical space with active learning. *J. Chem. Phys.* **2018**, *148*, 241733.
- (189) Smith, J.; Nebgen, B.; Zubatyuk, R.; Lubbers, N.; Devereux, C.; Barros, K.; Tretiak, S.; Isayev, O.; Roitberg, A. Approaching Coupled Cluster Accuracy with a General-purpose Neural Network Potential Through Transfer Learning. *Nat. Commun.* **2019**, *10*, 2903.
- (190) Devereux, C.; Smith, J. S.; Huddleston, K. K.; Barros, K.; Zubatyuk, R.; Isayev, O.; Roitberg, A. E. Extending the Applicability of the ANI Deep Learning Molecular Potential to Sulfur and Halogens. *J. Chem. Theory Comput.* **2020**, *16*, 4192–4202.
- (191) Zeng, J.; Tao, Y.; Giese, T. J.; York, D. M. QD $\pi$ : A Quantum Deep Potential Interaction Model for Drug Discovery. *J. Chem. Theory Comput.* **2023**, *19*, 1261–1275.
- (192) Pan, X.; Yang, J.; Van, R.; Epifanovsky, E.; Ho, J.; Huang, J.; Pu, J.; Mei, Y.; Nam, K.; Shao, Y. Machine-Learning-Assisted Free Energy Simulation of Solution-Phase and Enzyme Reactions. *J. Chem. Theory Comput.* **2021**, *17*, 5745–5758.
- (193) Zheng, P.; Zubatyuk, R.; Wu, W.; Isayev, O.; Dral, P. O. Artificial intelligence-enhanced quantum chemical method with broad applicability. *Nat. Commun.* **2021**, *12*, 7022.
- (194) Gómez-Flores, C. L.; Maag, D.; Kansari, M.; Vuong, V.-Q.; Irle, S.; Gräter, F.; Kubař, T.; Elstner, M. Accurate Free Energies for Complex Condensed-Phase Reactions Using an Artificial Neural Network Corrected DFTB/MM Methodology. *J. Chem. Theory Comput.* **2022**, *18*, 1213–1226.
- (195) Böser, J.; Kubař, T.; Elstner, M.; Maag, D. Reduction pathway of glutaredoxin 1 investigated with QM/MM molecular dynamics using a neural network correction. *J. Chem. Phys.* **2022**, *157*, 154104.
- (196) Dral, P. O.; Zubatyuk, T.; Xue, B.-X. Learning from multiple quantum chemical methods:  $\Delta$ -learning, transfer learning, co-kriging, and beyond. In *Quantum Chemistry in the Age of Machine Learning*; Dral, P. O., Ed.; Elsevier, 2022; Chapter 21, pp 491–507.
- (197) Martin, Y. C. Experimental and pK prediction aspects of tautomerism of drug-like molecules. *Drug Discovery Today. Technol.* **2018**, *27*, 59–64.
- (198) Milletti, F.; Vulpetti, A. Tautomer Preference in PDB Complexes and its Impact on Structure-Based Drug Discovery. *J. Chem. Inf. Model.* **2010**, *50*, 1062–1074.